

# On the effective plate thickness of monolayer graphene from flexural wave propagation

Sung Youb Kim,<sup>1,a)</sup> and Harold S. Park<sup>2</sup>

<sup>1</sup>*School of Mechanical Engineering, Ulsan National Institute of Science and Technology, Ulsan 689-798, South Korea*

<sup>2</sup>*Department of Mechanical Engineering, Boston University, Boston, Massachusetts 02215, USA*

(Received 3 March 2011; accepted 7 August 2011; published online 15 September 2011)

We utilize classical molecular dynamics to study flexural, or transverse wave propagation in monolayer graphene sheets and compare the resulting dispersion relationships to those expected from continuum thin plate theory. In doing so, we determine that regardless of the chirality for monolayer graphene, transverse waves exhibit a dispersion relationship that corresponds to the lowest order antisymmetric (A0) mode of wave propagation in a thin plate with plate thickness of  $h = 0.104$  nm. Finally, we find that the achievable wave speeds in monolayer graphene are found to exceed those reported previously for single walled carbon nanotubes, while the frequency of wave propagation in the graphene monolayer is found to reach the terahertz range, similar to that of carbon nanotubes. © 2011 American Institute of Physics. [doi:10.1063/1.3633230]

## I. INTRODUCTION

Graphene has recently been discovered as the simplest two-dimensional crystal structure.<sup>1,2</sup> Since then, graphene has been intensely studied for its high electronic quality,<sup>3,4</sup> for its potential in nanocomposites,<sup>5</sup> for its remarkable mechanical strength,<sup>6</sup> for its excellent thermal transport properties,<sup>7,8</sup> and also for its potential as the basic building block of future nanoelectromechanical systems (NEMS).<sup>9–15</sup>

As a basic building block for NEMS, graphene shows particular promise for ultrasensitive detection of masses, forces, and pressure due to its combination of extremely low mass and extremely high mechanical stiffness.<sup>6,9,12</sup> In all of these sensing applications, graphene will be used as the sensing element, and therefore will undergo transverse oscillations at extremely high frequencies. Because of this, understanding the nature of transverse elastic wave propagation in monolayer graphene is of fundamental interest. Furthermore, this also demonstrates the need to determine whether well-established continuum mechanics relationships for thin plates<sup>16,17</sup> are able to describe the dispersion relationships for monolayer graphene.

There has previously been extensive theoretical and computational effort to study elastic wave propagation in both single and multi-walled carbon nanotubes using both continuum beam and shell theories<sup>18–23</sup> as well as discrete atomistic calculations.<sup>24–26</sup> In general, the continuum theories have been found to adequately describe the dispersion relationships of carbon nanotubes (CNTs) at low wave numbers, while modifications to the continuum theories, for example, using non-local enhancements,<sup>18,19,22,25</sup> have been found to be necessary at higher wave numbers to account for atomic-scale or microstructural effects. However, the literature on wave propagation in graphene monolayers is considerably less developed.<sup>27,28</sup>

Therefore, the major purpose of this work is to utilize classical molecular dynamics (MD) simulations, study flexural (transverse) wave propagation in monolayer graphene sheets, and compare the resulting dispersion relationships to those obtained using classical continuum thin plate theories.<sup>16,29</sup> We determine the effective plate thickness using dispersion relationships and find that regardless of the chirality of monolayer graphene, transverse waves exhibit a dispersion relationship that corresponds to the lowest order antisymmetric (A0) mode of wave propagation in a thin plate with plate thickness of  $h = 0.104$  nm.

## II. SIMULATION METHODOLOGY

For monolayer graphene, the MD simulations were performed on a rectangular monolayer of graphene with dimensions  $147.6 \text{ nm} \times 1.70 \text{ nm}$ , which consisted of 9600 carbon atoms. Periodic boundary conditions were utilized in the  $y$  (1.70 nm) direction to mimic an infinite graphene monolayer, while transverse waves propagated along the  $x$  (147.6 nm) direction.

We utilized the second generation Brenner potential (REBO-II) (Ref. 30) for all intralayer carbon-carbon interactions; the REBO-II potential takes the form<sup>18,30</sup>

$$E = \sum_i \sum_{j \neq i} (E_R(r_{ij}) - b_{ij} E_A(r_{ij})), \quad (1)$$

where  $r_{ij}$  is the distance between atoms  $i$  and  $j$ ,  $b_{ij}$  is the bond order function, which accounts for the effects of neighboring atoms on the bond strength, and  $E_A$  and  $E_R$  are attractive and repulsive functions, which take the form

$$E_R(r_{ij}) = f_c(r_{ij}) \left( 1 + \frac{Q}{r_{ij}} \right) A \exp(-\alpha r_{ij}), \quad (2)$$

$$E_A = f_c(r_{ij}) \sum_{n=1}^3 B_n \exp(-\beta_n r_{ij}), \quad (3)$$

<sup>a)</sup>Electronic mail: sykim@unist.ac.kr.

where  $f_c$  is a cut-off function, and the parameters  $Q$ ,  $A$ ,  $\alpha$ ,  $B$ , and  $\beta$  are parameters for the potential that are given by Brenner *et al.*<sup>30</sup> We note that this potential has been shown to accurately reproduce binding energies, force constants, and elastic properties of graphene and has been utilized in prior studies of wave propagation in CNTs.<sup>18,20</sup>

The MD simulations were performed where the system was initially at 0 K, i.e., no initial random velocities corresponding to a specific temperature was applied to the atoms. The simulations were performed using a time step of 0.5 femtoseconds (fs), where the MD equations of motion were integrated using a standard velocity Verlet time integrator, and where no external reservoir was utilized to control the temperature or pressure of the system. Because we did not explicitly control the system temperature during the simulation, the temperature of the system did increase slightly due to the addition of minute amounts of energy through the applied sinusoidal transverse displacements, as described below, to excite the flexural wave propagation. However, it was verified that temperature increases of less than 5 K were observed for all simulations, thus ensuring that the simulations were performed at effectively 0 K. While low-temperature quantum mechanical effects are not captured by classical MD, the key factor to ensure accuracy of the dispersion calculations is the elastic stiffness of graphene, which is well-captured by the REBO-II potential, and which is known to show little deviation from 0 K to room temperature.

In order to obtain the dispersion relationships, we follow the methodology described by Wang and Hu<sup>25</sup> and Hu *et al.*<sup>18</sup> To do so, we applied sinusoidal transverse displacements with different periods of oscillation  $T$  at one end of the graphene sheet, while atoms at the other end of the sheet were fixed; the amplitude of the input sinusoidal wave was 0.02 Å to ensure linear wave propagation. Upon propagating a transverse wave through the graphene monolayer, standing waves are formed by the superposition of the outgoing and reflected waves. From the formation of the standing waves, the propagation duration  $\Delta t$  of the wave from a point  $x_1$  to a point  $x_2$  along the monolayer can be written as

$$\Delta t = \frac{(t_{32} - t_{31}) + (t_{42} - t_{41}) + \dots + (t_{n2} - t_{n1})}{n - 2}, \quad (4)$$

where  $t_{32}$  is the time of the third peak of oscillation measured at  $x_2$ ,  $t_{31}$  is the time for the third peak of oscillation to reach  $x_1$ , and  $n$  is the total number of oscillation peaks considered, which is typically about 10.

In the present numerical examples,  $x_1$  corresponds to a point that is 3.94 nm from the end of the graphene sheet where the sinusoidal wave is input, while  $x_2$  corresponds to a point that is 7.87 nm from the end of the graphene sheet where the sinusoidal wave is input. We show in Fig. 1 the displacement time history at points  $x = 0$ , 3.94, and 7.87 nm for an input transverse wave of period  $T = 300$  fs; the time for different peaks of oscillation ( $t_{31}$ ,  $t_{32}$ , etc.) that are needed to evaluate the propagation duration  $\Delta t$  are labeled for clarity.

Once the propagation duration  $\Delta t$  is known, the phase velocity  $c$ , and the wave number  $k$ , which are required to calculate the dispersion relationship, can be found as

$$c = \frac{x_2 - x_1}{\Delta t}, \quad (5)$$

and

$$k = \frac{2\pi}{\lambda} = \frac{\omega T}{\lambda} = \frac{\omega}{c}, \quad (6)$$

where the angular frequency  $\omega$  is related to the period  $T$  by the relationship

$$\omega = \frac{2\pi}{T}. \quad (7)$$

### III. CONTINUUM THIN PLATE THEORY

We also discuss the results from the MD simulations within the context of dispersion relationships obtained for continuum thin plate theory by Lamb.<sup>16</sup> This comparison is made because the situation we have considered in our MD simulations, in which the graphene monolayer is infinite through usage of periodic boundary conditions in the direction transverse to the wave propagation, is similar to that of a Lamb wave propagating along an infinite thin plate.<sup>16</sup> We consider graphene to be a plate, rather than a membrane, because a membrane is defined as a thin structure that has a negligible bending modulus. However, unlike membranes, a plate can sustain bending deformation because its bending strength is comparable to its tensile and compressive strength. In the case of graphene, recent experimental<sup>31</sup> and theoretical studies<sup>32</sup> have clearly shown that its bending rigidity is not negligible compared to the Young's modulus. We note that recent theoretical work has examined the validity of the thin plate approximation for the bending deformation of graphene monolayers.<sup>17</sup>

The dispersion relationship for thin plates is given by Losin<sup>29</sup> and is written as

$$\frac{\tan \eta \alpha}{\tan \eta \beta} + \left( \frac{(1 - \beta^2)^2}{4\alpha\beta} \right)^{\pm 1} = 0, \quad (8)$$

where  $\alpha = ((v/v_l)^2 - 1)^{1/2}$  and  $\beta = ((v/v_s)^2 - 1)^{1/2}$ ;  $v_l$  is the longitudinal wave speed,  $v_s$  is the shear wave speed,  $v$  is the phase velocity,  $\eta = kh/2$ , where  $k$  is the wave number and  $h$  is the thickness of the plate, and where the positive power refers to the symmetric mode while the negative power refers to the antisymmetric mode of wave propagation. For the Brenner (REBO-II) potential that we have utilized in the present work,<sup>30</sup> the wave speeds were previously calculated by Arroyo and Belytschko<sup>32</sup> and found to be  $v_l = 19.47$  km/s,  $v_s = 10.69$  km/s.

We note that while there has been extensive interest in recent years in determining the effective continuum plate thickness  $h$  due to the similarity of carbon nanotubes and graphene sheets to thin plates or shells,<sup>32-39</sup> none of these studies has determined the effective plate thickness from wave propagation via thin plate dispersion relationships. We now discuss the dispersion relationships for graphene

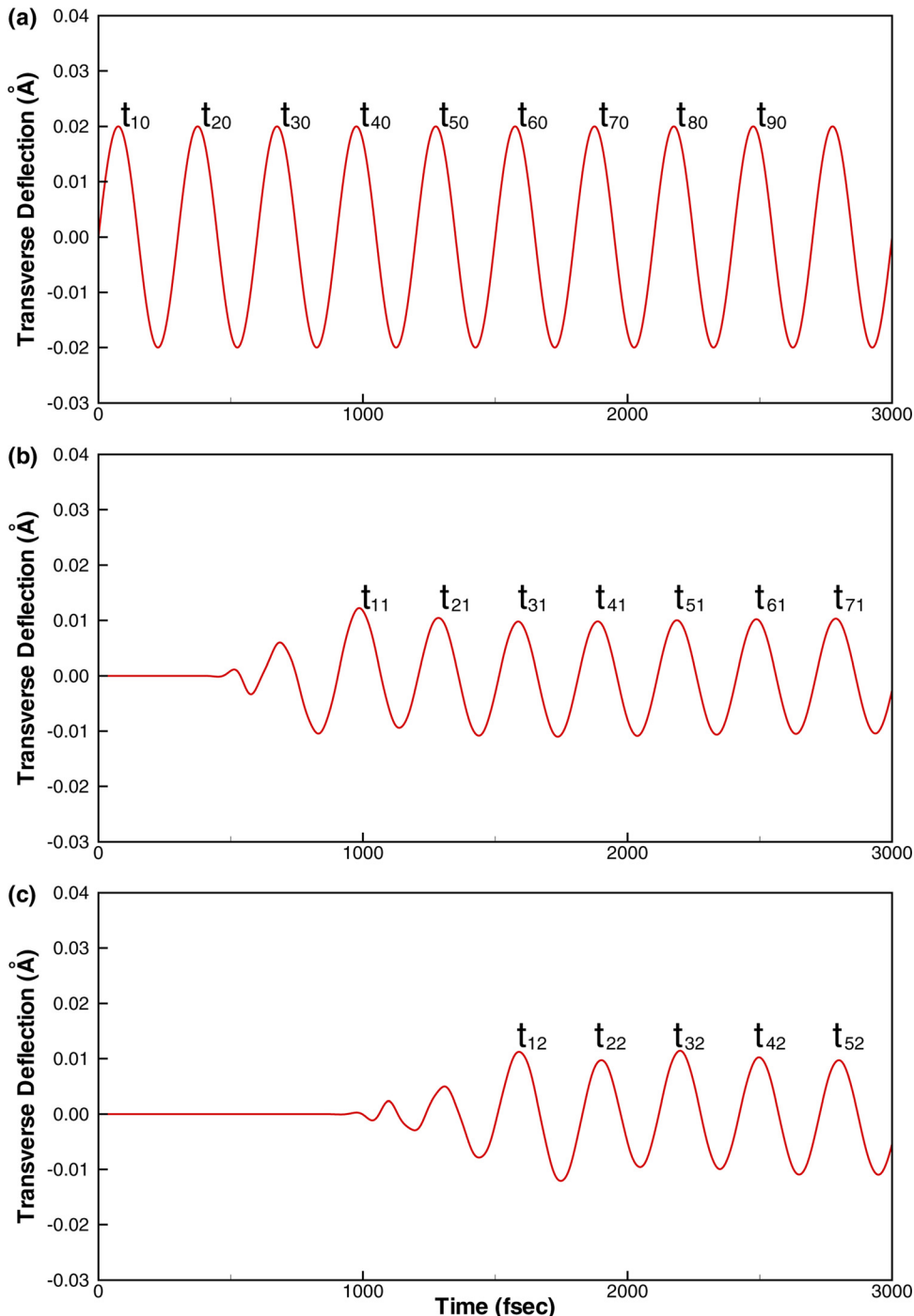


FIG. 1. (Color online) Time histories of the transverse deflection at different positions along the graphene monolayer. (a) The sinusoidal wave of period  $T = 300$  fs input at  $x = 0$ . (b) The deflection  $x = 3.94$  nm. (c) The deflection at  $x = 7.87$  nm.

monolayers and their relationships to those expected from continuum thin plate theory from the solution of Eq. (8).

#### IV. DISPERSION RESULTS FOR FLEXURAL WAVE PROPAGATION IN MONOLAYER GRAPHENE

The dispersion relationships for transverse wave propagation in a graphene monolayer are shown in Fig. 2; the results include those obtained from the MD simulations, and those obtained through solution of the continuum thin plate Eq. (8) assuming that monolayer graphene has an equivalent plate thickness of  $h = 0.07, 0.104$  and  $0.34$  nm. While excellent agreement is observed for the  $h = 0.104$  nm thickness

case, the relevance and meaning of all thicknesses will be discussed later.

Figure 2 demonstrates clearly that for transverse wave propagation in a graphene monolayer, significant dispersion, or dependence of the phase velocity upon the wave number, is observed at all wave numbers. In comparison to previously obtained results for carbon nanotubes, we find that graphene can support wave propagation at higher wave numbers than can nanotubes. This is not surprising as previous studies of flexural wave propagation in CNTs (Ref. 25) considered the transverse deflection or bending of CNTs. However, the equivalent mode of deformation for CNTs that corresponds to that excited in graphene in the present work would be a breathing mode of deformation, which can support shorter

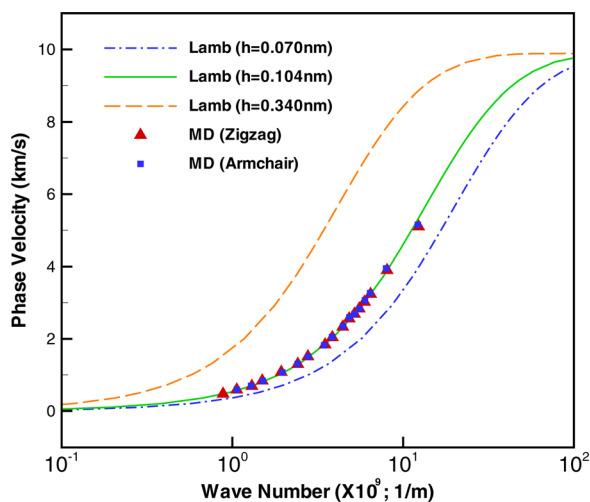


FIG. 2. (Color online) Comparison of dispersion relationships obtained using MD simulations and thin plate theory in Eq. (8) for both longitudinal and transverse wave propagation. The plate thickness for the continuum thin plate dispersion relationship in Eq. (8) is set as  $h = 0.07, 0.104, \text{ and } 0.34 \text{ nm}$ .

wavelengths than can the transverse bending mode of CNTs. For example, as reported by Wang and Hu,<sup>25</sup> the phase velocity begins to decrease for nanotubes at a wave number of about  $6 \times 10^9 \text{ m}^{-1}$  for (5,5) armchair nanotubes, and at a wave number of about  $2 \times 10^9 \text{ m}^{-1}$  for (10,10) armchair nanotubes. In contrast, graphene is observed in Fig. 2 to be able to support propagating transverse waves with wave numbers up to about  $15 \times 10^9 \text{ m}^{-1}$ , above which wave propagation is unable to occur.

The dispersion that occurs during transverse wave propagation in graphene is illustrated in Fig. 3. There, we show snapshots of the transverse wave propagation for input waves with a period ranging from 80 to 1000 fs. As is clearly observed in Fig. 3, severe dispersion is observed; higher frequency waves propagate with higher velocities than do lower frequency waves. While we note again that graphene can support transverse waves with higher wave numbers than can carbon nanotubes, the general shape of the dispersion relationship for monolayer graphene in Fig. 2 is quite similar to that reported for single walled carbon nanotubes.<sup>25</sup>

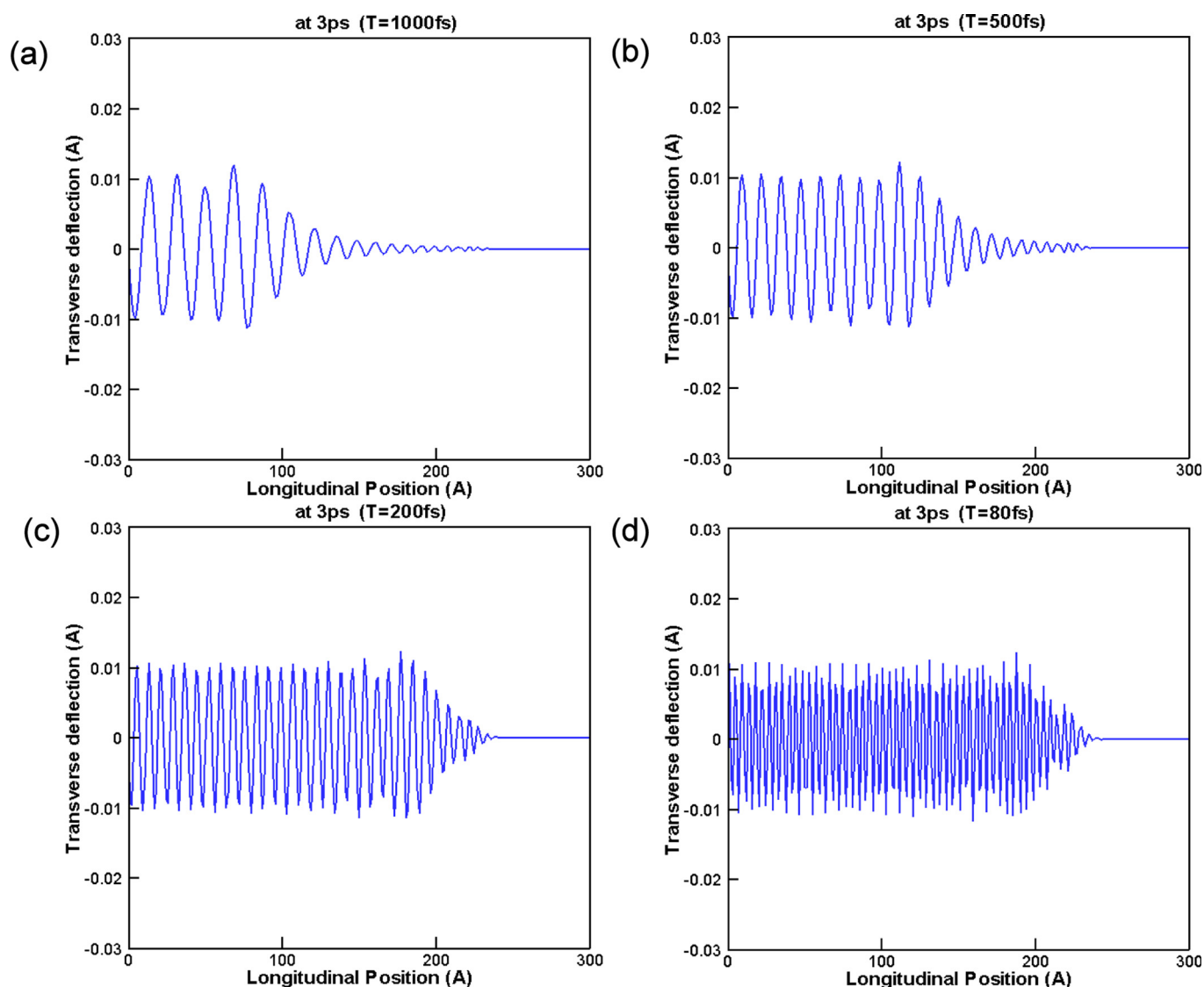


FIG. 3. (Color online) Snapshots of transverse wave propagation in graphene monolayer with different input periods ( $T$ ) of oscillation at time = 3 ps.



### A. Comparison of MD results with continuum thin plate theory for monolayer graphene

As discussed earlier, Fig. 2 showed the dispersion relationships obtained both from MD simulations and also from the solution of the continuum thin plate Eq. (8). As previously shown in Eq. (8), one of the key parameters in the continuum thin plate dispersion relationship is the variable  $\eta = kh/2$ , where  $k$  is the wave number and  $h$  is the plate thickness. The continuum plate theory dispersion results shown in Fig. 2 were obtained by setting the plate thickness  $h = 0.104$  nm; for that value of plate thickness, the MD dispersion relationship exactly matches the continuum thin plate dispersion relationship for transverse waves, or the lowest order antisymmetric mode (A0) of wave propagation, for all wave numbers for which wave propagation is supported by monolayer graphene. Furthermore, a similar agreement is observed for wave propagation along both the armchair and zigzag directions of monolayer graphene.

For comparison, we also show results obtained by assuming different thicknesses of graphene as also seen in Fig. 2. In particular, we choose two additional values of interest. First, Fig. 2 also shows results assuming that the thickness of a graphene monolayer is  $h = 0.34$  nm. This value has been used extensively in continuum shell theory approximations of nanotubes and graphene<sup>39</sup> and corresponds to the interlayer thickness in multilayer graphene sheets or multi-walled carbon nanotubes. If the dispersion relationships from the MD simulations are scaled by this thickness, the trends match those from Eq. (8) for transverse wave propagation. However, the curves do not align, which clearly demonstrates that setting the thickness of the monolayer graphene sheet to be  $h = 0.34$  nm is incorrect.

We also show results in Fig. 2 assuming that the thickness of the graphene monolayer is  $h = 0.07$  nm; this value was chosen as it represents an average of the thickness range of 0.05 to 0.09 nm that is typically used in continuum shell theories for nanotubes and graphene.<sup>39</sup> As seen in Fig. 2, choosing the thickness to be 0.07 nm also leads to discrepancies in comparison to the MD dispersion relationships, as the transverse phase velocity is underpredicted. The results in Fig. 2 thus indicate that for the presently utilized Brenner potential,<sup>30</sup> the correct plate thickness is about  $h = 0.104$  nm for transverse wave propagation.

We also place the effective plate thickness of  $h = 0.104$  nm of graphene in the context of previous studies of carbon nanotubes and graphene<sup>28,32–38</sup>; an extensive study and analysis of these approaches is given by Huang *et al.*<sup>39</sup> By fitting results obtained from atomistic simulations of either tension or bending to continuum shell theory, an effective nanotube thickness of about 0.05–0.09 nm has been reported;<sup>39</sup> as recently observed by Huang *et al.*,<sup>39</sup> this thickness depends both on the interatomic potential utilized, as well as the loading methodology. The effective thickness reported here ( $h = 0.104$  nm for transverse wave propagation) is close to the range of values reported previously, while emphasizing that, to the best of the authors' knowledge, the effective continuum plate thickness for monolayer graphene has not been determined previously from dispersion relationships.

There are additional points that should be noted in comparing the dispersion relationships obtained from MD and from continuum thin plate theory. For example, in the high wave number limit in continuum thin plate theory, the transverse wave speeds approach the Rayleigh wave speed. However, due to the discrete, atomic nature of the graphene monolayer, we find through the MD simulations that for transverse wave propagation, waves with wavelength smaller than about 3.88 Å are unable to propagate through the graphene monolayer. Therefore, the Rayleigh wave speed is unattainable in graphene monolayers; this explains why there are no data points from the MD simulations at high wave numbers in Fig. 2. However, because of the similarity between the MD and continuum dispersion relationships, we report that the Rayleigh speed in the graphene sheet, which represents the limiting value of the phase velocity as the wave number increases in Fig. 2, would be about 9.89 km/s.

### V. CONCLUSIONS

In conclusion, we have utilized classical molecular dynamics to obtain the dispersion relationships for flexural or transverse wave propagation in monolayer graphene sheets. One key finding is that continuum thin plate theory well approximates the dispersive behavior for flexural wave propagation in monolayer graphene. Furthermore, for the presently utilized interatomic potential,<sup>30</sup> we have found that regardless of the chirality, if the graphene monolayer is assumed to have a thickness of  $h = 0.104$  nm, the dispersion relationships obtained from the molecular dynamics simulations agree with those obtained from continuum thin plate theory for transverse wave propagation.

### ACKNOWLEDGMENTS

H.S.P. also acknowledges support from NSF Grant No. CMMI-0750395. S.Y.K. acknowledges support from the National Research Foundation of Korea (KRF) grant funded by the Korea Government (MEST) (Grant No. 2011-0013440) and the PLSI supercomputing resources of KISTI. Both authors acknowledge Professor Sulin Zhang for sharing his Brenner code.

<sup>1</sup>K. S. Novoselov, A. K. Geim, S. V. Morozov, D. Jiang, M. I. Katsnelson, I. V. Grigorieva, S. V. Dubonos, and A. A. Firsov, *Nature* **438**, 197 (2005).

<sup>2</sup>K. S. Novoselov, D. Jiang, F. Schedin, T. J. Booth, V. V. Khotkevich, S. V. Morozov, and A. K. Geim, *Proc. Natl. Acad. Sci. U.S.A.* **102**, 10451 (2005).

<sup>3</sup>A. K. Geim and K. S. Novoselov, *Nature Mater.* **6**, 183 (2007).

<sup>4</sup>A. H. C. Neto, F. Guinea, N. M. R. Peres, K. S. Novoselov, and A. K. Geim, *Rev. Mod. Phys.* **81**, 109 (2009).

<sup>5</sup>S. Stankovich, D. A. Dikin, G. H. B. Dommett, K. M. Kohlhaas, E. J. Zimney, E. A. Stach, R. D. Piner, S. T. Nguyen, and R. S. Ruoff, *Nature* **442**, 282 (2006).

<sup>6</sup>C. Lee, X. Wei, J. W. Kysar, and J. Hone, *Science* **321**, 385 (2008).

<sup>7</sup>S. Ghosh, W. Bao, D. L. Nika, S. Subrina, E. P. Pokatilov, C. N. Lau, and A. A. Balandin, *Nature Mater.* **9**, 555 (2010).

<sup>8</sup>J. H. Seol, I. Jo, A. L. Moore, L. Lindsay, Z. H. Aitken, M. T. Pettes, X. Li, Z. Yao, R. Huang, D. Broido, N. Mingo, R. S. Ruoff, and L. Shi, *Science* **328**, 213 (2010).

<sup>9</sup>J. S. Bunch, A. M. van der Zande, S. S. Verbridge, I. W. Frank, D. M. Tanenbaum, J. M. Parpia, H. G. Craighead, and P. L. McEuen, *Science* **315**, 490 (2007).

- <sup>10</sup>D. Garcia-Sanchez, A. M. van der Zande, A. S. Paulo, B. Lassagne, P. L. McEuen, and A. Bachtold, *Nano Lett.* **8**, 1399 (2008).
- <sup>11</sup>J. T. Robinson, F. K. Perkins, E. S. Snow, Z. Wei, and P. E. Sheehan, *Nano Lett.* **8**, 3137 (2008).
- <sup>12</sup>J. S. Bunch, S. S. Verbridge, J. S. Alden, A. M. V. D. Zande, J. M. Parpia, H. G. Craighead, and P. L. McEuen, *Nano Lett.* **8**, 2458 (2008).
- <sup>13</sup>S. Y. Kim and H. S. Park, *Nano Lett.* **9**, 969 (2009).
- <sup>14</sup>S. Y. Kim and H. S. Park, *Appl. Phys. Lett.* **94**, 101918 (2009).
- <sup>15</sup>R. A. Barton, B. Ilic, A. M. van der Zande, W. S. Whitney, P. L. McEuen, J. M. Parpia, and H. G. Craighead, *Nano Lett.* **11**, 1232 (2011).
- <sup>16</sup>H. Lamb, *Proc. R. Soc. London* **93**, 114 (1917).
- <sup>17</sup>D.-B. Zhang, E. Akatyeva, and T. Dumitrica, *Phys. Rev. Lett.* **106**, 255503 (2011).
- <sup>18</sup>Y.-G. Hu, K. M. Liew, Q. Wang, X. Q. He, and B. I. Yakobson, *J. Mech. Phys. Solids* **56**, 3475 (2008).
- <sup>19</sup>Q. Wang, *J. Appl. Phys.* **98**, 124301 (2005).
- <sup>20</sup>C. Y. Wang, C. Q. Ru, and A. Mioduchowski, *Phys. Rev. B* **72**, 075414 (2005).
- <sup>21</sup>T. Natsuki, M. Endo, and H. Tsuda, *J. Appl. Phys.* **99**, 034311 (2006).
- <sup>22</sup>K. M. Liew and Q. Wang, *Int. J. Eng. Sc.* **45**, 227 (2007).
- <sup>23</sup>J. Yu, R. K. Kalia, and P. Vashista, *J. Chem. Phys.* **103**, 6697 (1995).
- <sup>24</sup>C. Li and T.-W. Chou, *Phys. Rev. B* **73**, 245407 (2006).
- <sup>25</sup>L. Wang and H. Hu, *Phys. Rev. B* **71**, 195412 (2005).
- <sup>26</sup>K. M. Liew, Y. A. Hu, and X. Q. He, *J. Comput. Theor. Nanosci.* **5**, 581 (2008).
- <sup>27</sup>S. Narendar, D. R. Mahapatra, and S. Gopalakrishnan, *Comput. Mater. Sci.* **49**, 734 (2010).
- <sup>28</sup>F. Scarpa, M. Ruzzene, S. Adhikari, and R. Chowdhury, *Proc. SPIE* **7646**, 76461A (2010).
- <sup>29</sup>N. A. Losin, *J. Vib. Acoust.* **123**, 417 (2001).
- <sup>30</sup>D. W. Brenner, O. A. Shenderova, J. A. Harrison, S. J. Stuart, B. Ni, and S. B. Sinnott, *J. Phys.: Condens. Matter* **14**, 783 (2002).
- <sup>31</sup>T. J. Booth, P. Blake, R. R. Nair, D. Jiang, E. W. Hill, U. Bangert, A. Bleloch, M. Gass, K. S. Novoselov, M. I. Katsnelson, A. K. Geim, *Nano Lett.* **8**, 2442 (2008).
- <sup>32</sup>M. Arroyo and T. Belytschko, *Phys. Rev. B* **69**, 115415 (2004).
- <sup>33</sup>B. I. Yakobson, C. J. Brabec, and J. Bernholc, *Phys. Rev. Lett.* **76**, 2511 (1996).
- <sup>34</sup>J. P. Lu, *Phys. Rev. Lett.* **79**, 1297 (1997).
- <sup>35</sup>Z. Xin, Z. Jianjun, and O.-Y. Zhong-can, *Phys. Rev. B* **62**, 13692 (2000).
- <sup>36</sup>Z.-C. Tu and Z.-C. Ou-Yang, *Phys. Rev. B* **65**, 233407 (2002).
- <sup>37</sup>A. Pantano, D. M. Parks, and M. C. Boyce, *J. Mech. Phys. Solids* **52**, 789 (2004).
- <sup>38</sup>L. Wang, Q. Zhang, J. Z. Liu, and Q. Jiang, *Phys. Rev. Lett.* **95**, 105501 (2005).
- <sup>39</sup>Y. Huang, J. Wu, and K. C. Hwang, *Phys. Rev. B* **74**, 245413 (2006).